

APPLICATION OF TIME-FREQUENCY DECOMPOSITION METHOD IN THE STUDY OF GAS RESERVOIR IN THE SERGIPE-ALAGOAS BASIN

Alexandre de J. Pinho and Milton J. Porsani

ABSTRACT. The sedimentary basin of Sergipe-Alagoas, located on the Brazilian east bank, presents one of the most complete stratigraphic sections of the Brazilian continental margin. Hydrocarbon exploration activities began more than 50 years ago. The recent discoveries of hydrocarbons (gas and oil of high API grade) in turbiditic reservoirs of deep waters have further awakened the exploratory interest of the basin. Problems related to the processing and interpretation of seismic data have always received great attention from the scientific community. Currently, the use of time-frequency decomposition methods of the seismic signal is of great interest. Spectral decomposition has been widely used in reservoir characterization, such as determination of layer thickness, stratigraphic visualization with seismic attributes and identification of low frequency anomalies associated with the presence of gas. The mechanism causing these anomalies is not yet well known, but they are often attributed to the high attenuation of gas filled reservoirs. The approach used for spectral decomposition combines the maximum entropy method and the Wigner-Ville distribution, based on the idea of the Burg method that uses the prediction error operator to extend the Wigner-Ville kernel sequences by applying the Fourier transform to each extended sequence, thus allowing to obtain the Wigner-Ville distribution of maximum entropy.

Keywords: Sergipe-Alagoas Basin, Wigner-Ville distribution, maximum entropy, spectral decomposition, seismic attributes, low frequency anomaly.

RESUMO. A bacia sedimentar de Sergipe-Alagoas, localizada na margem leste brasileira, apresenta uma das mais completas seções estratigráficas da margem continental brasileira. As atividades exploratórias de hidrocarbonetos foram iniciadas há mais de 50 anos. As recentes descobertas de hidrocarbonetos (gás e óleo de elevado grau API) em reservatórios turbidíticos de águas profundas despertaram ainda mais o interesse exploratório da bacia. Os problemas relacionados ao processamento e à interpretação de dados sísmicos sempre receberam grande atenção da comunidade científica. Atualmente, desperta grande interesse o uso de métodos de decomposição tempo-frequência do sinal sísmico. A decomposição espectral tem sido bastante utilizada na caracterização de reservatório, como estimativa de espessura de camada, visualização estratigráfica com atributos sísmicos e identificação de anomalias de baixa frequência que podem estar associadas à presença de gás. O mecanismo causador dessas anomalias ainda não é perfeitamente conhecido, mas é frequentemente atribuído a atenuação das altas frequências nos reservatórios preenchidos com gás. A abordagem utilizada para a decomposição espectral combina o método de máxima entropia e a distribuição de Wigner-Ville, com base na ideia do Método de Burg que usa o operador de erro de predição para estender as sequências do kernel de Wigner-Ville aplicando a transformada de Fourier para cada sequência estendida, permitindo assim, obter a distribuição Wigner-Ville de máxima entropia.

Palavras-chave: Bacia Sergipe-Alagoas, distribuição Wigner-Ville, máxima entropia, decomposição espectral, atributos sísmicos, anomalia de baixa frequência.

INTRODUCTION

The stratigraphic traps associated to the Calumbi turbidites present high exploratory risks due to the absence of a structural control that normally assists in the accumulation of petroleum. The identification of these reservoirs using seismic attributes, such as the instantaneous average frequency, can minimize the uncertainties that are inherent to this type of trap.

Problems related to the processing and interpretation of seismic data have always received great attention from the scientific community. Currently, the use of time-frequency decomposition methods of the seismic signal is of great interest. This important and current topic is of great interest to the oil industry. The study on the suitability and feasibility of the time-frequency representation method in the identification of hydrocarbon reservoirs in the Sergipe-Alagoas Basin represents the main challenge to be studied in this work.

In seismic exploration, spectral decomposition refers to any method that produces a continuous time-frequency analysis of the seismic data (Castagna, 2006). Therefore, for each sample of the seismic time there is a frequency spectrum. There are a variety of spectral decomposition methods, such as: Discrete Fourier Transform, Fast Fourier Transform, Wigner-Ville Maximum Entropy, Continuous Wavelet Transform (Zoukanéri & Porsani, 2015).

The temporal and frequency resolution of the time-frequency decomposition is important for the application of the method. Resolution is the ability to accurately map the time and frequency of occurrence of an event.

The most popular of time-frequency representations is the spectrogram. This type of representation is in general obtained from the Short Time Fourier Transform (STFT) technique. A window is used to obtain temporal resolution. In contrast, in order to obtain good resolution in frequency, a long window is required. This process of window selection is the main limitation of STFT due to Heisenberg's uncertainty principle.

The S-transform and Gabor transform are other types of transform that have been proposed in order to overcome such a problem of resolution associated with the windows. There is also the use of transformers based on the use of wavelet (continuous and discrete wavelet transform) and others that use the projection of the signal on a predefined dictionary (Matching-pursuit and Basis-pursuit).

There are also other alternative methods that utilize a family of functions (Cohen class functions) that are bilinear time-frequency representation of the signal energy density (Cohen, 1989; Choi & Williams, 1989; Zoukanéri, 2014). The Wigner-Ville Distribution (WVD) is the simplest and principal member of this

family and exhibits a large amount of mathematical properties that are desired and, in addition, demonstrates good time-frequency resolution.

THEORY

One way to accomplish the time-frequency decomposition is through the so-called quadratic or bilinear functions. This classification is due to the fact that the signal to be analyzed is introduced twice in the decomposition generating a square matrix of energy density. The set of techniques that make use of the quadratic function was summed up by Cohen (1989), reason why these decompositions are denominated bilinear functions of the class of Cohen. The general formulation of Cohen's class functions is represented in the form:

$$C(t, f) = \iiint_{-\infty}^{+\infty} g_1\left(t + \frac{x_0}{2}\right) g_2\left(t - \frac{x_0}{2}\right) \times \phi(t - \varepsilon, f - \mu) e^{-jpf x_0} dx_0 d\varepsilon d\mu \quad (1)$$

where $g_1(\cdot)$ and $g_2(\cdot)$ are temporal or spatial series; x_0 is a displacement of the variable t ; f is the frequency and $\phi(\cdot, \cdot)$ is the kernel. ε and μ are the displacement of the variable associated with the kernel.

Equation (1) is a convolution consisting essentially of two parts: the first one is characterized by a covariance matrix and can be expressed as:

$$\int_{-\infty}^{+\infty} g_1\left(t + \frac{x_0}{2}\right) g_2\left(t - \frac{x_0}{2}\right) dx_0 \quad (2)$$

and the second part consists of a distribution kernel and given by:

$$\int_{-\infty}^{+\infty} (t - \varepsilon, f - \mu) e^{-j\pi f x_0} d\varepsilon d\mu \quad (3)$$

The time-frequency decompositions of the Cohen class can be seen as a translation of the matrix covariance in time and frequency convoked by a weight function constituted by the kernel.

The different expressions taken by the kernel characterize the type or name of the distribution. If $\phi(t, f) = \delta(t, f)$, the expression is equivalent to the Wigner-Ville distribution, explained in the next section. This distribution constitutes the most basic of the bilinear energy density distributions of the Cohen class.

In Equation (1), the signs of $g_1(\cdot)$ and $g_2(\cdot)$ may be real or complex, same or different, but in the case of Wigner-Ville they become analytical signs. In the strategy adopted by Zoukanéri (2014), a single analytical signal was used.

Distribution of Wigner-Ville

The Wigner-Ville Distribution (WVD) is a three-dimensional decomposition of a time series (time-frequency and energy) introduced by Eugen Wigner in 1932 (Wigner, 1932 apud Zoukanéri, 2014) to study the problem of static equilibrium in the area of quantum mechanics. Wigner's works were completed in 1948 by J. Ville (Ville, 1948 apud Zoukanéri, 2014) and applied in signal analysis.

The discrete form of WVD is a powerful tool for representing and analyzing chirp signals. The obtained representation has a high resolution in the time-frequency domain even in the case of signals whose frequency changes rapidly with time. The Wigner Ville distribution of a signal $x(t)$ is given by:

$$W(t, f) = \int_{-\infty}^{+\infty} z\left(t + \frac{\tau}{2}\right)z^*\left(t - \frac{\tau}{2}\right)e^{-i\pi f\tau} d\tau \quad (4)$$

From Equation (4), it is noted that the WV distribution is the Fourier Transform (FT) of the elements of the covariance function $z(t + t/2)z^*(t - t/2)$. Thus, as a consequence, the WV distribution satisfies the properties of FT, among others. The most relevant properties are quoted below.

1. The WVD is always real since it always represents the Fourier transform of the product of Hermitian functions (real part even and odd part imaginary).
2. Integration over time results in the power spectrum of the signal and is called the marginal frequency distribution.

$$\int_{-\infty}^{+\infty} W(t, f)dt = |z(f)|^2 \quad (5)$$

3. Frequency integration results in the energy spectrum of the signal and is called the time domain distribution.

$$\int_{-\infty}^{+\infty} W(t, f)df = |z(t)|^2 \quad (6)$$

4. The integration along frequency and time represents the total energy of the signal (this guarantees the conservation of energy).

$$Ez = \frac{1}{2\pi} \iint_{-\infty}^{+\infty} W(t, f)dt df \quad (7)$$

A change in the time or frequency of the signal implies the same change in distribution.

$$g(t) = f(t - to)W_g(t, f) = W_f(t - to, f) \quad (8)$$

$$G(f) = F(f - fo)W_G(t, f) = W_f(t - to, f) \quad (9)$$

The WVD is fully invertible, that is, the covariance matrix of the signal, given by the product $z(t + \tau/2)z^*(t - \tau/2) = r_z(t, \tau)$ can be retrieved through the inverse Fourier transform

$$r_z(t, \tau) = \frac{1}{2\pi} \int_{-\infty}^{+\infty} W_z(t, f)e^{i\pi f\tau} df \quad (10)$$

The matrix $r_z(t, \tau)$ is Hermitian and of unit rank. Using the first eigenvector and eigenvalue it is possible to recover the input signal z :

$$Z(t) = \sqrt{(\lambda_1)}u_1(t) \quad (11)$$

where λ_1 is the first eigenvector and u_1 the first eigenvalue.

The marginal properties 2 and 3 together with property 6 indicate whether a two-variable function satisfies the WV distribution. Figure 1 shows the Wigner-Ville decomposition and the marginal conditions represented by the instantaneous energy in Figure 1b and the power spectrum in Figure 1d.

Attenuation of interference terms

WVD computing of a multicomponent function introduces interferences due to cross-terms. This is due to the fact that WVD is a quadratic function. Several methods have been proposed to attenuate the terms of interference and make WVD an efficient tool for signal analysis. Attenuation has two objectives:

- (i) Smoothing out interference terms;
- (ii) Maintaining the concentration of components in the time and frequency domain (i.e. maintaining the resolution of the representation).

One method that proved capable of satisfying the two conditions is the combination of the Discrete Wigner-Ville theory with Burg's Maximum Entropy method.

Maximum Entropy Method

In the estimation of the power spectrum, the Short Time Fourier Transform (STFT) of the coefficients of the Autocorrelation Function (ACF) is commonly used. However, the use of the Fourier transform is limited by the effects of leakage when the data are truncated. A solution to obtain a good resolution from a limited series of data was formulated by Burg (1975 apud

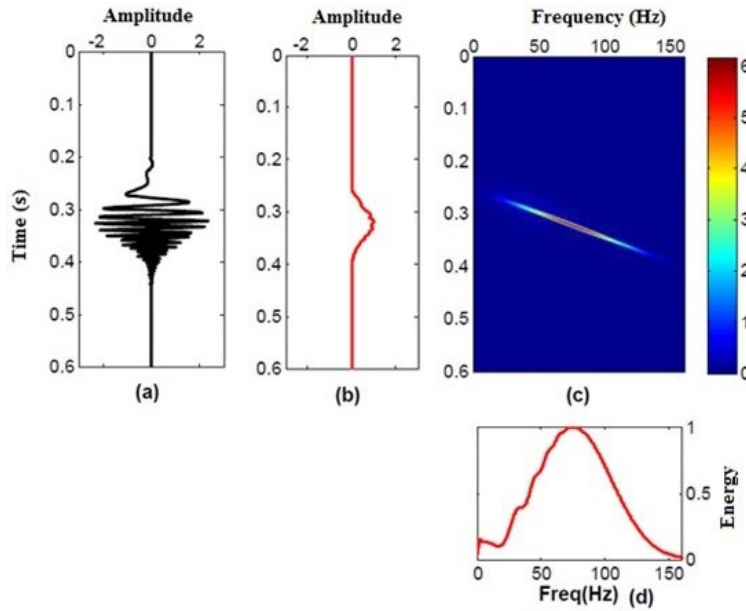


Figure 1 – Wigner-Ville decomposition and the marginal properties. (a) synthetic signal, (b) marginal property in frequency: instantaneous energy, (c) Wigner-Ville distribution, (d) marginal property in time: power spectrum (Zoukanéri, 2014).

Zoukanéri 2014) by the Maximum Entropy Method. The entropy of a Gaussian process is proportional to:

$$\int_{-f_N}^{+f_N} \log P(f)df \quad (12)$$

where $P(f)$ is the power spectrum, and f_N is the Nyquist frequency. Burg maximizes the entropy with the following condition:

$$R_n = \int_{-f_N}^{+f_N} P(f) \exp(i2\pi fn\Delta t)df \quad (13)$$

where R_n is the autocovariance, $-N < n < N$.

The solution is obtained using the Lagrange coefficients $\lambda_k, k = 1, \dots, N$, such that

$$\begin{aligned} & \frac{\partial}{\partial P(f)} \left(\int_{-f_N}^{+f_N} \log P(f)df \right) \\ & - \lambda_k \left(\sum_{-M}^M P(f) \exp(i2\pi fn\Delta t) \right) = 0 \end{aligned} \quad (14)$$

The solution to Equation (14) is given by:

$$P(f) = \frac{E_{N_c-1} \Delta t}{\left| \sum_{n=0}^{N_c-1} c_n e^{-i2\pi fn\Delta t} \right|^2} \quad (15)$$

where $P(f)$ is the power spectrum, $c_n, n = 0, \dots, N_c - 1, (c_0 = 1)$, represents the coefficients of the prediction error

operator (PEO) of order N_c, E_{N_c} is the energy error counterpart, f is bounded by the Nyquist interval $-1/2\Delta t \leq f \leq 1/2\Delta t$.

Equation (15) is considered the basic expression of the Maximum Entropy Method. The power spectrum $P(f)$ is completely defined if the coefficients c_n and the energy E_{N_c} are known. Several methods can be used to determine the PEO coefficients of order N_c and the corresponding energy. Among the most used is the Burg algorithm (1967 apud Zoukanéri, 2014). This method is based on the least squares criterion.

Maximum entropy method applied to WVD

The idea is to use the Burg method to compute the PEO and then use the PEO coefficients to compute and extend each Wigner-Ville kernel sequence. The spectrum obtained through this procedure avoids the effects of the interference terms of the classic Wigner-Ville representation.

To each sequence of $K(n)$ it is possible to associate an analytic signal $\tilde{z}(n)$ whose boundaries will be defined by a window L . The sequence of autocorrelation coefficients corresponding to $\tilde{z}(n)$ is:

$$\tilde{z}(n) = \left\{ z\left(n - \frac{L}{2}\right), \dots, z(n), \dots, z\left(n + \frac{L}{2}\right) \right\} \quad (16)$$

where L is an odd number representing a symmetric time window and centered at the point $z(n)$. The window size L and the

number of coefficients of the N_c filter control the resolution of the decomposition in the time-frequency plane.

The sequence of autocorrelation coefficients corresponding to $\tilde{z}(n)$ is:

$$\tilde{K}(n) = \left\{ k\left(n - \frac{L}{2}\right), \dots, k(n), \dots, k\left(n + \frac{L}{2}\right) \right\} \quad (17)$$

Using the Burg algorithm to obtain ACF coefficients associated with the maximum entropy spectrum, one can apply the $\tilde{K}(n)$ by stating its coefficients as:

$$\tilde{k}_n(j) = - \sum_{i=1}^{j-1} \tilde{k}_n(j-i)c(j-1, i) - c(j, j)E_{j-1} \quad (18)$$

From the Hermitian properties of the kernel we have $\tilde{k}_n(-j) = \tilde{k}_n^*(j)$. Using Equation (18), the terms $\tilde{k}_n(j), j = 1, \dots, N_c$ are calculated. The remainder of the terms $N_c < j \leq N$ are obtained by imposing $c(j, j) = 0$. It is observed that Equation (18) allows to estimate both the odd and even part of the kernel. The instantaneous power density spectra of the Wigner-Ville distribution is obtained by making the Discrete Fourier Transform of Equation (18).

By shutting down the window and repeating the process for all kernel sequences, the time-frequency representation of Wigner-Ville Maximum Entropy Method (WV-MEM) is achieved without the influence of the interference terms.

Extraction of instantaneous attributes

The instantaneous frequency is commonly estimated from the complex trace, through the derivative of the instantaneous phase. This estimate, however, is quite susceptible to noise. As a way of overcoming the noise, the average instantaneous frequency can be obtained by computing the first moment of the Wigner-Ville distribution (Boashash, 1992 apud Zoukanéri, 2014). Its expression is given by:

$$\hat{f}(t) = \frac{\int_{-\infty}^{+\infty} fW(t, f)df}{\int_{-\infty}^{+\infty} W(t, f)df} \quad (19)$$

where \hat{f} is the instantaneous average frequency, f is the frequency, $W(f, t)$ is the Wigner-Ville distribution obtained with the WV-MEM.

Equation (19) suggests that the instantaneous frequency is the weighted average curve of the Wigner-Ville distribution. The frequency thus calculated is more stable to noise. Equation (19) also suggests that the Wigner-Ville spectrum is first computed in the Fourier domain. However, using the Parseval theorem and the symmetries of the power spectrum, is possible to compute the

instantaneous average frequency directly in the time domain as presented in Zoukanéri & Porsani (2015).

$$\hat{f}(n) = \frac{2 \sum_{l=1}^{l=(N-1)/2} q(l)\hat{K}_n(l)}{NK_n(0)} \left(\frac{1}{N\Delta t} \right) \quad (20)$$

where $\hat{f}(n)$ is the instantaneous average frequency, $q(l)$ is the imaginary part of the inverse Fourier transform of the sawtooth function (Weber & Arfken, 2003), $\hat{K}_n(l) = \text{Imag}(\hat{K}_n(l))$ is the imaginary part of the terms of the sequence $\tilde{k}(n)$ obtained from Eq. (18). The term $1/N\Delta t$ is required to convert to frequency unit.

In addition to frequency, higher order attributes can also be estimated. The second moment of WV-MEM is related to the local deviation of the frequencies with respect to the average frequency. This deviation is called the Instant Bandwidth and is given by:

$$\sigma^2(t) = \frac{\int_{-\infty}^{+\infty} (f - \hat{f}(t))^2 W(t, f)df}{\int_{-\infty}^{+\infty} W(t, f)df} \quad (21)$$

In the same way the third and fourth moments are related respectively to the skewness and the attribute kurtosis. Skewness describes the deviation of the density function with respect to normal and is given by the expression:

$$S(t) = \frac{\int_{-\infty}^{+\infty} (f - \hat{f}(t))^3 W(t, f)df}{\sigma^3(t) \int_{-\infty}^{+\infty} W(t, f)df} \quad (22)$$

It indicates the degree of asymmetry or distance from the normal measure, that is, it quantifies how symmetrical a distribution is (Fig. 2). A symmetric (Gaussian) distribution, by default, has a zero skewness. An asymmetric distribution with a long tail to the right (values higher than normal) has skewness positive (inclination facing the negative side). Already an asymmetric distribution with a long tail to the left will have a negative skewness (i.e., a slope facing the positive side).

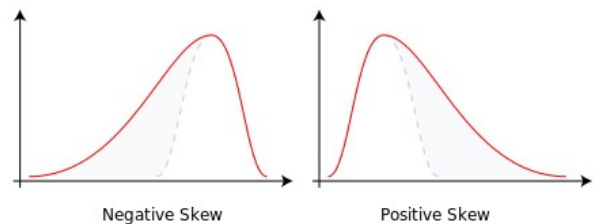


Figure 2 – Graphical representation of asymmetry distribution (skewness).

Meanwhile, kurtosis measures how sharp (peakness) is the distribution. This attribute is computed from the WV-MEM as:

$$K(t) = \frac{\int_{-\infty}^{+\infty} (f - \hat{f}(t))^4 W(t, f)df}{\sigma^4(t) \int_{-\infty}^{+\infty} W(t, f)df} - 3 \quad (23)$$

where the term -3 causes $K(t)$ to take zero value for a normal distribution case.

The sharper the shape of the wavelet in the seismic trait, the closer it is to the reflectivity. Therefore, it is called kurtosis to the degree of flattening of a distribution with respect to the degree of a normal (Gaussian) distribution that is taken as the standard.

Although it is common to explain kurtosis as the degree of flattening of a frequency distribution, what the measures of kurtosis actually seek to indicate is the degree of concentration of values of the distribution around the center of this distribution.

In a unimodal distribution, the greater the concentration of values around the center of the same, the greater the value of its kurtosis. Graphically, this will be associated with a curve with the sharper central part, showing a more prominent, more pointed peak frequency, characterizing the mode of distribution more clearly (Fig. 3).

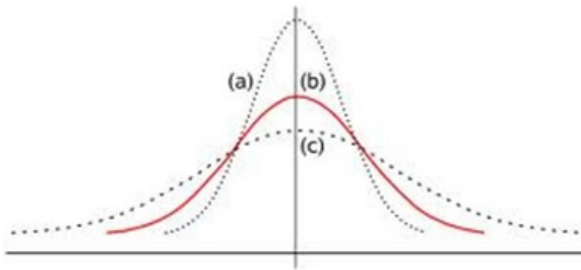


Figure 3 – Graphical representation of different flattening degrees of a distribution (kurtosis).

Low Frequency Anomaly

Low frequency anomalies have been observed since the late 1970s (Taner et al., 1979). There are numerous examples of successes of frequency analysis as indicative of hydrocarbon (Castagna, 2003; Korneev et al., 2004; Sinha et al., 2005; Goloshubin et al., 2006).

The mechanism for generating low frequency shading zones below gas reservoirs is still not well known. These anomalies are usually associated with high attenuation of high frequencies in gas-bearing reservoirs. However, this fact is difficult to explain in thin reservoirs, where the propagation time of the wave along the attenuating medium is small.

Tai et al. (2009) suggests for these cases that only the presence of low-speed zones would cause the low frequency zones below the reservoirs. According to Goloshubin et al. (2006), there are several types of low frequency anomaly. In some cases, these anomalies are located in the reservoir itself, without a delay in the seismic time in relation to the reflector corresponding to the reservoir.

In other cases, the anomalies are located with a seismic delay of more than a hundred milliseconds below the reservoir. For

Goloshubin et al. (2006), this delay is due to the conversion of the fast-slow-fast P -wave into interlaminated (thickness less than one m) and highly permeable reservoir.

The slow P wave is associated with the mobility of fluids relative to the porous framework. As this wave is greatly attenuated, it is usually ignored in the exploration seismic, but for this geological model has to be considered.

Many authors use the attenuation concept to justify low frequency because the phenomenon of attenuation is as if it were operating a low pass filter that suppresses high frequencies proportionally more than the low frequencies.

Some oil/gas reservoirs usually have a low value of Q (quality factor) than the surrounding rocks and thus exhibit an anomalous zone of absorption (Tai et al., 2009). Even so, it is difficult to explain the anomalies observed on little thick reservoirs where there is not enough time of travel of the waves on the reservoirs with gas that justifies such anomaly (Castagna, 2003).

According to Tai (2009), if the low frequency anomaly is caused simply by attenuation factors, then it is possible to compensate the high frequency components within the anomaly by applying a reverse filter of Q . However, Wang (2007) showed that the low frequency shadow zone continues to exist even after the Q compensation.

The paper published by Tai (2009) seeks to explain the physical reasons for the correlation of the presence of gas in thin reservoirs and the low frequency anomaly. He classified the frequency influence factors into two categories. The first, which he called global factors, groups the frequency changes into every seismic section and determines the background frequency. Wavelet, the adopted flowchart of seismic data processing, and regional geological structures, for example, are part of this group.

The other category, which he classified as local factors, includes, for example, the variation of thickness, the variation of local properties of lithofacies and the presence of abnormal pressure in the pores of the reservoir.

In the study of local factors, Tai (2009) found a relationship between reservoir thickness, velocity and density with the low frequency anomaly that can be summarized as follows: Reservoir thickness and acoustic impedance are the main factors controlling the spectral response of the seismic signal in a and if the thickness of the reservoir varies less than 20%, velocity is the dominant factor that influences the frequency variation.

RESULTS

The objective of this work is the deep water reservoirs. They are part of the supersequence that marks the beginning of the drift phase of the basin. Sediment deposition occurred initially in a

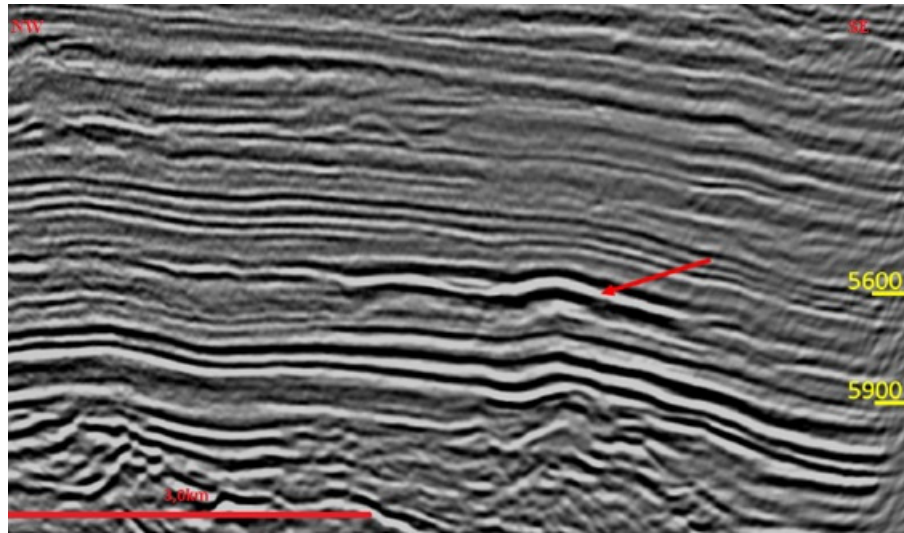


Figure 4 – Zoom in Section VB-24. Red arrow indicates reservoir position of the Calumbi Formation. Seismic reflectors with high amplitude, around the time 5900 ms, represent the marine generating rock of Continguiaba Formation.

restricted marine environment that later evolved into an open sea environment as the oceanic crust set in. This supersequence is composed by the Sergipe Group (Riachuelo and Continguiaba Formations) and Piaçabuçu Group (Calumbi, Marituba and Mosqueiro Formations) (Araújo, 2009).

According to Feijó (1994), the Calumbi Formation consists of gray to greenish argillite and shales, with intercalations of fine and coarse sandstones. Argillite and shales would have been deposited on the slope and on the abyssal plain, while the sandstones are interpreted as being of currents of turbidity currents.

The turbidite sandstones are the reservoirs that were used in the studies of the low frequency anomalies associated with the accumulation of gas. To test the effectiveness of the method on real data we have used two seismic lines and drilled wells that pass over the reservoirs. The anomaly was studied using the instantaneous average frequency obtained through WV-MEM. In addition, we also analyzed the behavior of the attributes instantaneous energy, kurtosis and skewness.

The first line (called VB-24) has direction NW-SE (dip direction of the basin). It has about 58 km of extension. It passes through a turbidite reservoir bearing gas in the seismic time of approximately 5570 ms on the 5500 trace. The top of the reservoir is highlighted by a low acoustic impedance anomaly (white peak in seismic) (Fig. 4). In this section is also possible to observe the marine generating rock of the basin represented by the amplitude anomaly around the time 5900 ms.

An instantaneous average frequency profile of the trace passing over the reservoir is shown in Figure 5. Figure 5b represents

the time-frequency plane with the curve marking the variation of the instantaneous average frequency of the trace. The instantaneous energy was plotted over frequency curve. The red peaks on the frequency curve represent the points associated with the high energy.

In Figure 5b, the black arrow indicates the top of the reservoir. Therefore, it is possible to observe that this point of the reservoir marks an anomaly of high instantaneous energy (associated to the high amplitude) and that, along the reservoir, the frequency decays, being the base of the reservoir represents a place of low instantaneous average frequency.

Figures 6 and 7, respectively, represent the overlapping of the instantaneous average frequency section over the seismic amplitude and the instantaneous energy section also over the seismic amplitude. The blue color reveals the low frequency sites (ranging from 0 to 16 Hz). The low frequency anomalies associated with the presence of gas occur just below the reservoir (Fig. 6).

The attribute skewness establishes, as seen, the degree of asymmetry of a distribution in relation to the Gaussian distribution. A positive skewness represents a distribution where its peak is relatively close to the origin, i.e., the elements with the highest frequencies are the ones with the lowest values of the distribution.

Figure 8 shows the behavior of skewness in the study section. It is possible to verify that on the base of the gas-bearing reservoir is where the highest values of the attribute are recorded. The higher the value of skewness, the more positive is the asymmetry. A higher positive asymmetry is related, in our case, to the lower

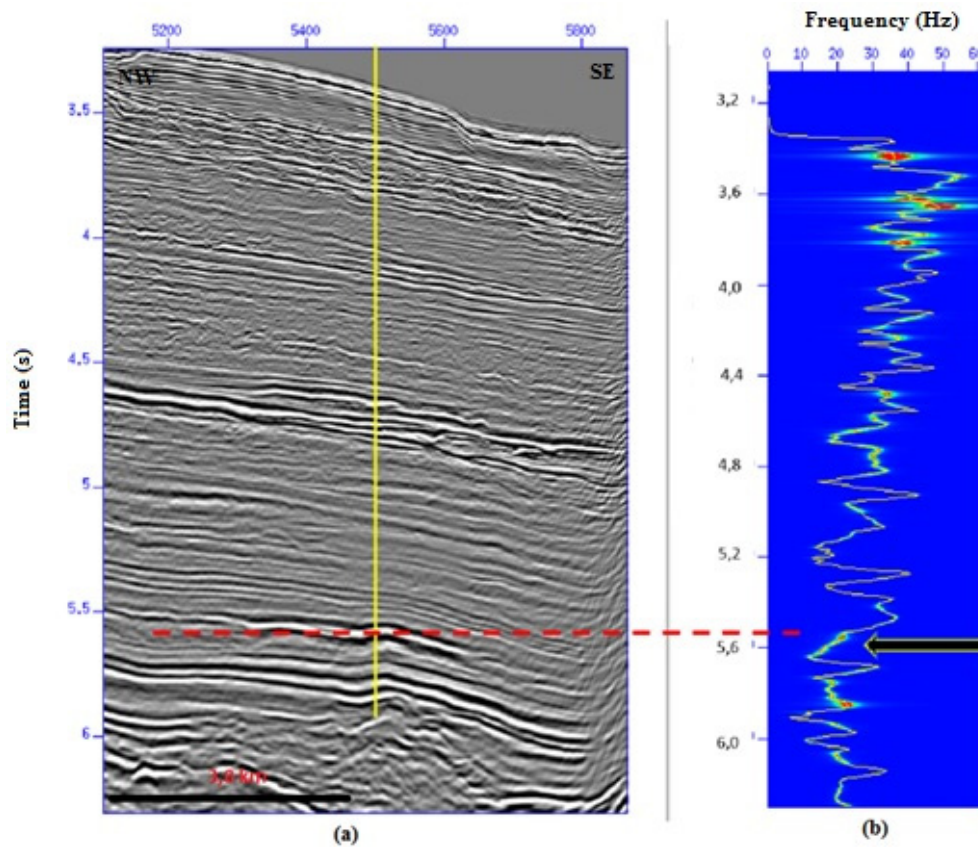


Figure 5 – Section VB-24 showing the position of the profile of the instantaneous average frequency over the 5500 trace, (b) represents the time-frequency plane of the trace showing the variation of frequency and high energy points (red peaks). The black arrow indicates the top of the reservoir.

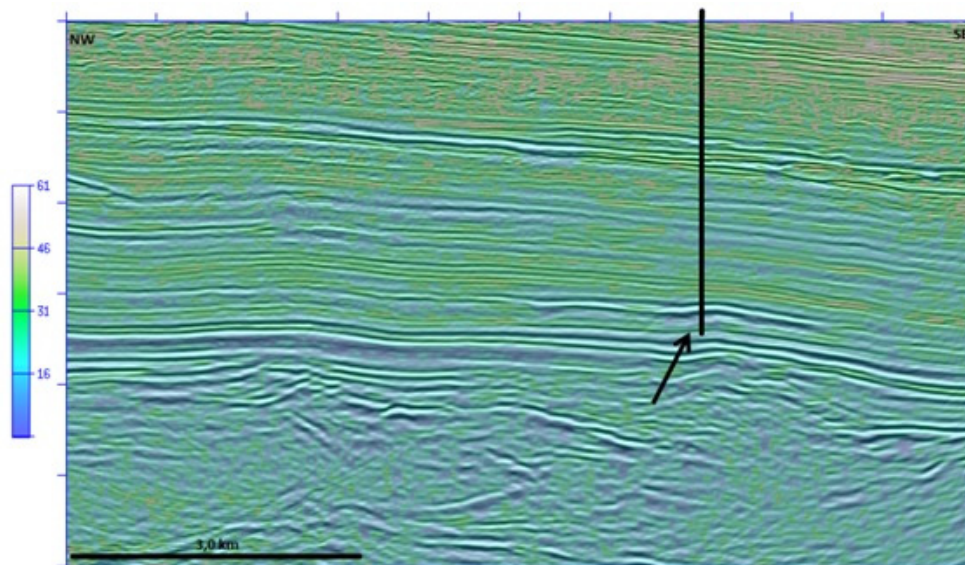


Figure 6 – Section VB-24 with the instantaneous average frequency (transparency of 50 percent) on the seismic amplitude. The black arrow indicates the anomaly low frequency occurring below the gas reservoir.

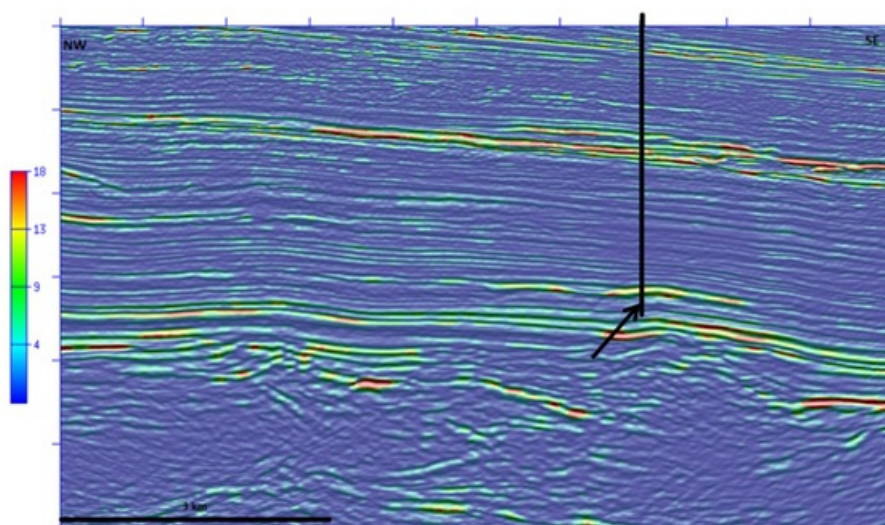


Figure 7 – Section VB-24 with the instantaneous energy (transparency of 50 percent) on the seismic amplitude. The gas-carrying reservoir is a region where the highest instantaneous energy values occur (yellow and red).

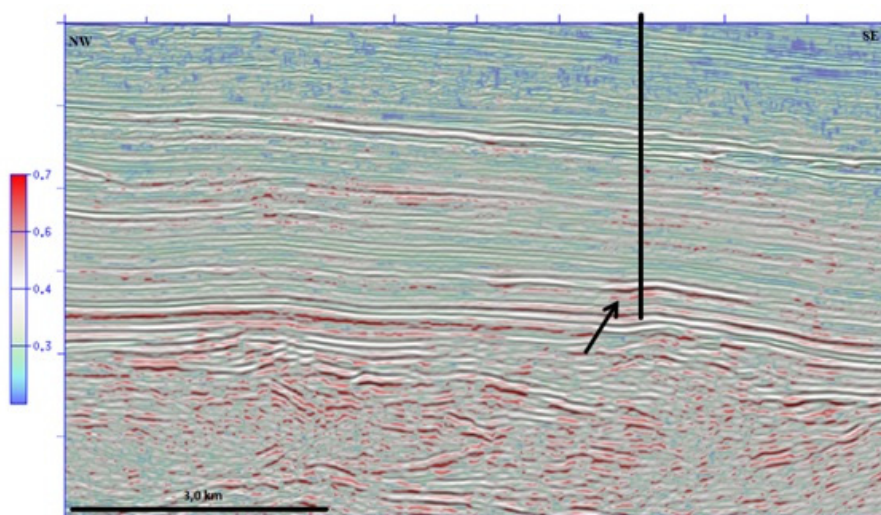


Figure 8 – Section VB-24 with the attribute skewness (transparency of 50 percent) on the seismic amplitude. The arrow indicates the base of the reservoir where marks a region of high skewness values associated with low frequencies.

frequency bands. That is, the skewness attribute is an indirect way of studying, in this case, the behavior of the instantaneous average frequency.

Kurtosis stipulates how pointy a distribution is compared to a normal (Gaussian) distribution. The kurtosis measurements indicate the degree of concentration of the values of the distribution. So, a relatively high value indicates that there is concentration of the values around the center. However, the smaller values indicate a dispersion of the distribution around its center.

From the analysis of Figure 9, it is concluded that the base

of the Calumbi Formation reservoir is a region where high values of kurtosis are concentrated, that is, below the reservoir the distribution is more pointed. This means that there is no dispersion of distribution values in that region. This behavior was expected since, based on the frequency investigation, the base of this is a region of low frequency concentration, thus, this behavior is reflected in the high values of kurtosis. The kurtosis attribute is also an indirect way of studying the behavior of the frequency.

The second line tested was SA232. It has direction (NE-SW) parallel to the strike direction of the Basin. It has about 30 km

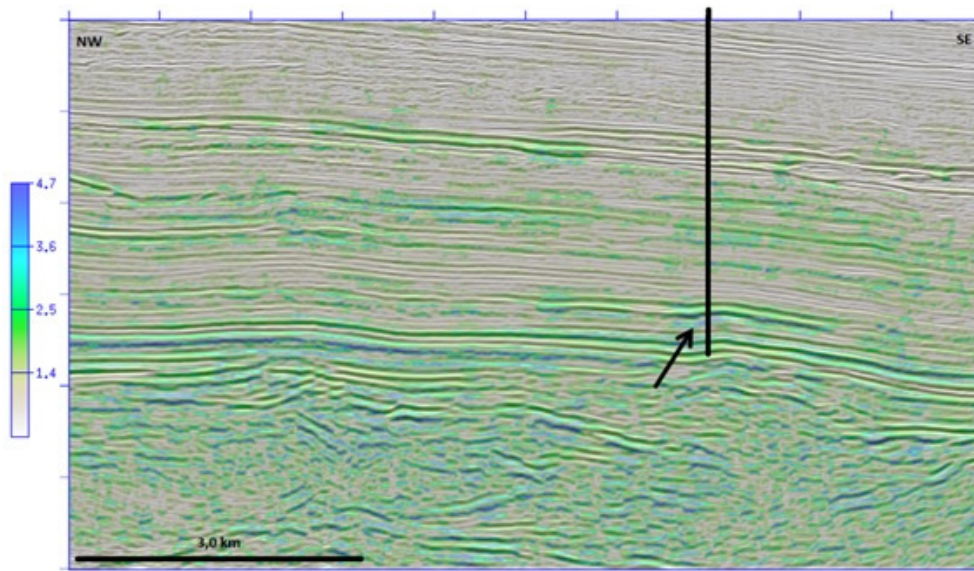


Figure 9 – Section VB-24 with the attribute kurtosis (transparency of 50 percent) on the seismic amplitude. The arrow indicates the base of the reservoir region of high kurtosis values associated distribution (concentration of the values of the near the center).

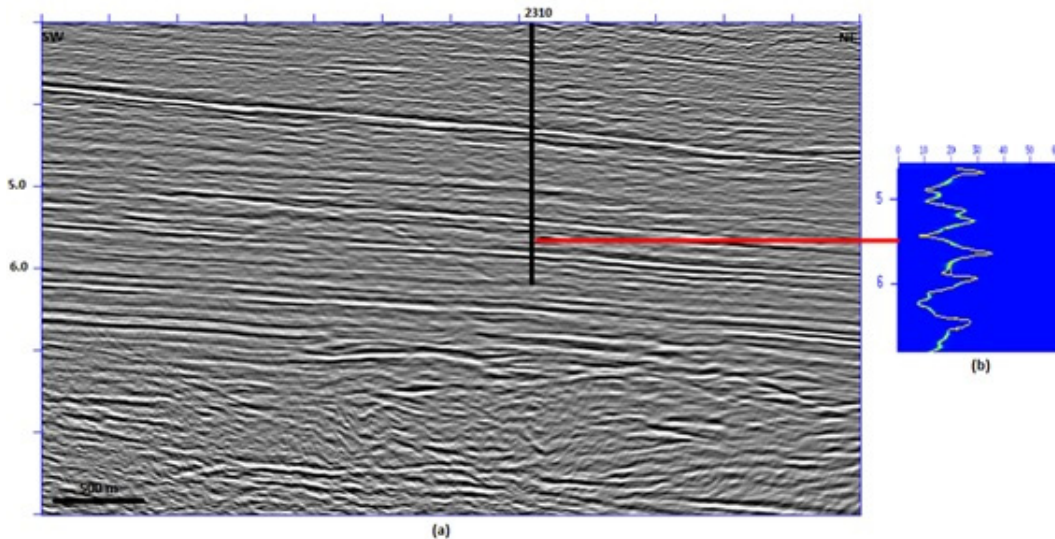


Figure 10 – (a) Section SA232 showing the position of the profile extraction of the frequency. (b) Time-frequency plot of the trace showing the variation of the instantaneous average frequency curve. About this same curve was plotted the peaks of the instantaneous energy (red color).

of extension. This seismic line contains a well that drilled a turbiditic reservoir saturated with water (Fig. 10). It is noted, once again, that the top of the reservoir is marketed by an anomaly of low acoustic impedance (white peak in seismic).

Trace 2310 passes over the reservoir (Fig. 10b). This graph, which represents the time-frequency decomposition of the trace, does not show the low frequency anomaly associated with the gas accumulations, i.e., there is no reduction in the value of

the characteristic instantaneous average frequency over the reservoir with its base being a local low frequency. The instantaneous energy, which is plotted over frequency curve, apparently did not indicate the top of the reservoir as a high energy point.

The frequency and energy behavior responses suggest the absence of gas (Figs. 11 and 12). The attributes skewness (Fig. 13) and kurtosis (Fig. 14) have different responses when compared to the responses obtained in the reservoir with asso-

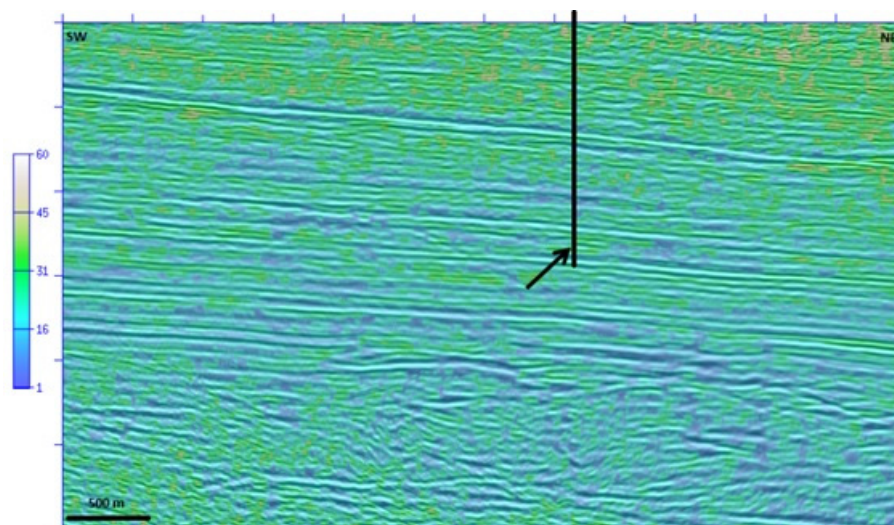


Figure 11 – Section SA232 with the instantaneous average frequency (transparency of 50 percent) on the seismic amplitude. The arrow indicates the region below the reservoir where there is no occurrence of low frequencies.

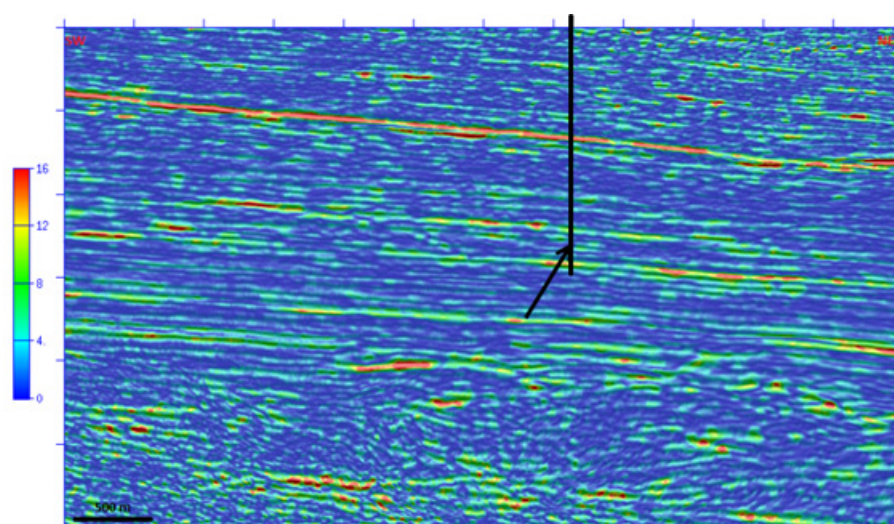


Figure 12 – Section SA232 with the instantaneous energy (transparency of 50 percent) over the seismic amplitude.

ciated gas. In the case of skewness, the positive asymmetry does not correspond to the highest values of this attribute (above 0.6 in the scale). The kurtosis also resulted in values different from those obtained in the gas reservoirs, thus generating a distribution with more values around the center (less pointed).

CONCLUSIONS

The approach used for spectral decomposition combines the maximum entropy method and the Wigner-Ville distribution, based on the idea of the Burg method that uses the prediction error operator to extend the Wigner-Ville kernel sequences by apply-

ing, then, the Fourier transform to each extended sequence of the kernel, thus allowing to obtain the Wigner-Ville distribution of maximum entropy.

The instantaneous average frequency was obtained directly in the time domain using the proposed method (WV-MEM). This frequency is obtained with a derivative operator applied to the Wigner-Ville Maximum Entropy Kernel. The high temporal and frequency resolution are fundamental aspects that value it, besides the robustness of the method against noise, compared to traditional methods. The number of coefficients (the order of the operator N_c) and the window L , used to estimate the prediction operator, control the resolution of the method.

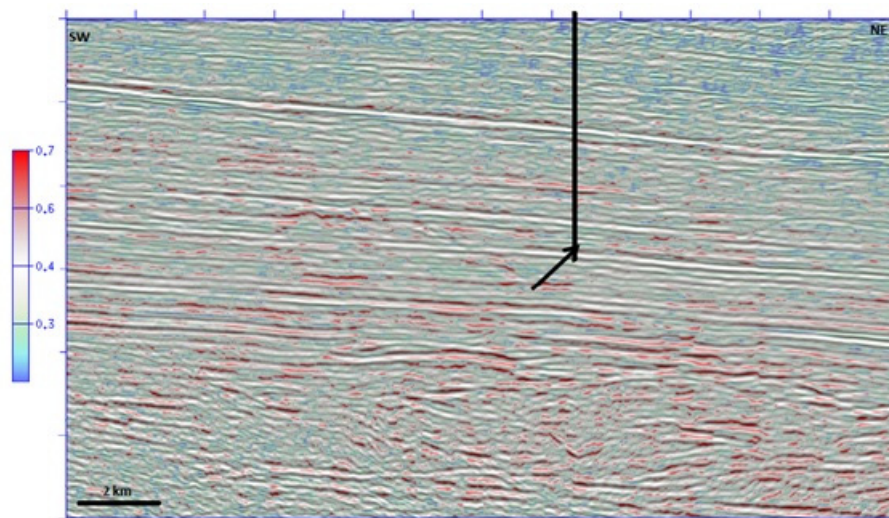


Figure 13 – Section SA232 with the attribute skewness (transparency of 50 percent) on the seismic amplitude. The arrow indicates the base where there is no characteristic presence of the highest values of asymmetry associated with lower frequency.

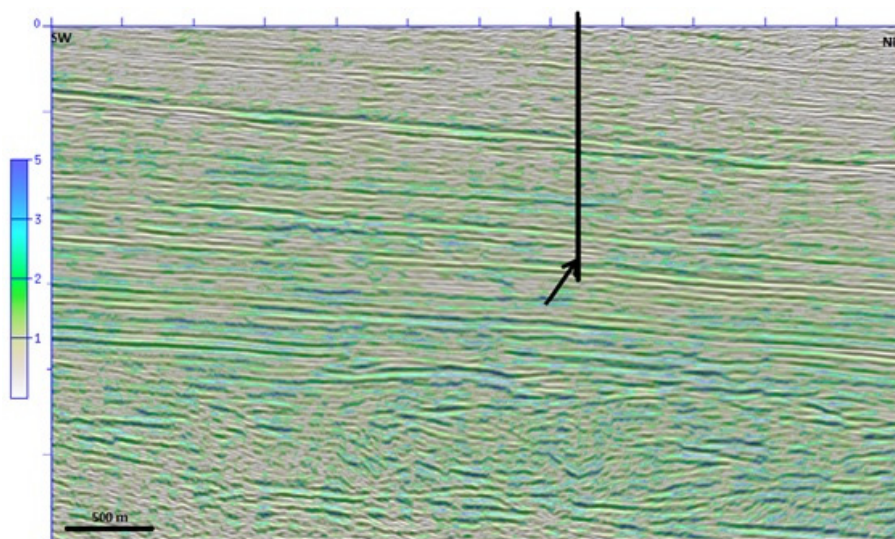


Figure 14 – Section SA232 with the attribute kurtosis (transparency of 50 percent) on the seismic amplitude. The arrow indicates the base of the reservoir where low values are associated with a distribution less sharply (i.e. there is a dispersion of their central value).

The location of an exploratory well, when the main objective is a stratigraphic trap, requires much more studies to minimize the exploratory risks. The application of the instantaneous average frequency studies, in this case, has helped to minimize the risks of prospecting by observing the low frequency anomalies that are associated with the presence of gas.

The use of higher order attributes, such as skewness and kurtosis, served as a criterion for quality control of the studied anomalies. In addition, these attributes improved the resolution of the anomalies studied (they more accurately marked the be-

havior of the anomaly below the reservoir) in a significant way that is even possible to infer the extension of the reservoir more precisely.

ACKNOWLEDGMENT

The authors thank ANP (Agência Nacional do Petróleo, Gás Natural e Biocombustíveis) for providing the data set and the permission for academic purposes. The authors also thank INCT-GP/CNPq/MCT, FINEP, FAPESB for financial support.

REFERENCES

- ARAÚJO CC. 2009. Carbonatos aptianos do campo Carmópolis, bacia Sergipe-Alagoas: Estratigrafia e modelo deposicional. *Boletim de Geociências da Petrobras*, 17(2): 311–330.
- BURG JP. 1967. Maximum entropy spectral analysis. In: *Proceedings of 37th Meeting, Society of Exploration Geophysicists, Oklahoma City*.
- BURG JP. 1975. Maximum entropy spectrum analysis. Doctorate Thesis. Stanford University. 246 pp.
- CASTAGNA JP. 2006. Comparison of spectral decomposition methods. *First Break, Society of Exploration Geophysicists*, 24(3): 75–79.
- CASTAGNA JP, SUN SJ & SIEGFRIED RW. 2003. Instantaneous spectral analysis: Detection of low-frequency shadows associated with hydrocarbons. *The Leading Edge*, 22(120): 124–127.
- CHOI HI & WILLIAMS WJ. 1989. Improved time-frequency representation of multi-component signals using exponential kernels. *IEEE Transactions on Acoustics, Speech and Signal Processing*, 37: 862–871, doi: 10.1109/ASSP.1989.28057.
- COHEN L. 1989. Time-frequency distributions – A review. *Proceedings of the IEEE*, 77: 941–981, doi: 10.1109/5.30749.
- FEIJÓ FJ. 1994. Bacias de Sergipe e Alagoas. *Boletim de Geociências da Petrobras*, 8(1): 149–161.
- GOLOSHUBING, KORNEEV V, VANSCHUYVER C, SILIN D & VINGALOV V. 2006. Reservoir imaging using low frequencies of seismic reflections. *The Leading Edge*, 25(5): 527–531.
- KORNEEV V, GOLOSHUBIN G, VAMSCHUYVER C & SILIN D. 2004. Seismic low-frequency effects in monitoring of fluid-saturated reservoirs. *Geophysics*, 69: 522–532.
- SINHA SK, ROUTH PS, ANNO PD, PHILLIPS C & CASTAGNA JP. 2005. Spectral decomposition of seismic data with continuous-wavelet transform. *Geophysics*, 70: 19–25. doi: 10.1190/1.2127113.
- TAI S, PURYEAR C & CASTAGNA JP. 2009. Local frequency as a direct hydrocarbon indicator. In: *SEG Houston 2009 International Exposition and Annual Meeting, Houston, Texas*, p. 2160–2164.
- TANER MT, KOEHLER F & SHERIFF RE. 1979. Complex seismic trace analysis. *Geophysics*, 44: 1041–1063.
- ZOUKANÉRI IM. 2014. Análise tempo-frequência do sinal sísmico utilizando a Distribuição Wigner-Ville e o Método de Máxima Entropia: Aplicações para estimativa do fator Q e de atributos. Doctorate Thesis. Pós-Graduação em Geofísica. Instituto de Geociências, Universidade Federal da Bahia, Salvador, Brazil, 48 pp.
- ZOUKANÉRI IM & PORSANI MJ. 2015. A combined Wigner-Ville and maximum entropy method for high-resolution time-frequency analysis of seismic data. *Geophysics*, 80(6): 01–011.
- WANG Y. 2007. Seismic time-frequency spectral decomposition by matching pursuit. *Geophysics*, 72(1): V13–V20.
- WEBER HJ & ARFKEN GB. 2003. *Essential Mathematical Methods for Physicists*. Academic Press. USA, 932 pp.

Recebido em 13 dezembro, 2017 / Aceito em 4 julho, 2018
 Received on December 13, 2017 / Accepted on July 4, 2018